AGE (2012) 34:805–819
DOI 10.1007/s11357-011-9281-x

Skeletal muscle contractile function and neuromuscular performance in *Zmpste24*$^{-/-}$ mice, a murine model of human progeria

Sarah M. Greising · Jarrod A. Call · Troy C. Lund · Bruce R. Blazar · Jakub Tolar · Dawn A. Lowe

Received: 25 January 2011 / Accepted: 14 June 2011 / Published online: 29 June 2011

Abstract Human progeroid syndromes and premature aging mouse models present as segmental, accelerated aging because some tissues and not others are affected. Skeletal muscle is detrimentally changed by normal aging but whether it is an affected tissue in progeria has not been resolved. We hypothesized that mice which mimic Hutchinson–Gilford progeria syndrome would exhibit age-related alterations of skeletal muscle. *Zmpste24*$^{-/-}$ and *Zmpste24*$^{+/+}$ littermates were assessed for skeletal muscle functions, histo-morphological characteristics, and ankle joint mechanics. Twenty-four-hour active time, ambulation, grip strength, and whole body tension were evaluated as markers of neuromuscular performance, each of which was at least 33% lower in *Zmpste24*$^{-/-}$ mice compared with littermates ($p<0.06$). Contractile capacity of the posterior leg muscles were not affected in *Zmpste24*$^{-/-}$ mice, but muscles of the anterior leg were 30–90% weaker than those of *Zmpste24*$^{+/+}$ mice ($p<0.01$). Leg muscles were 32–47% smaller in the *Zmpste24*$^{-/-}$ mice and contained ~60% greater collagen relative to littermates ($p<0.01$). Soleus and extensor digitorum longus muscles of *Zmpste24*$^{-/-}$ mice had excessive myonuclei and altered fiber size distributions but, otherwise, appeared normal. Ankle range of motion was 70% lower and plantar- and dorsiflexion passive torques were nearly 3-fold greater in *Zmpste24*$^{-/-}$ than *Zmpste24*$^{+/+}$ mice ($p\leq0.01$). The combined factors of muscle atrophy, collagen accumulation, and perturbed joint mechanics likely contributed to poor neuromuscular performance and selective muscle weakness displayed by *Zmpste24*$^{-/-}$mice. In summary, these characteristics are similar to those of aged mice indicating accelerated aging of skeletal muscle in progeria.

Keywords Aging · Lamin · Range of motion · Sarcopenia · Strength

Abbreviations

EDL	Extensor digitorum longus
HGPS	Hutchinson–Gilford progeria syndrome
P_o	Maximal isometric tetanic force
ROM	Range of motion

S. M. Greising · J. A. Call · D. A. Lowe
Rehabilitation Science and Program in Physical Therapy,
University of Minnesota, School of Medicine,
420 Delaware Street SE,
Minneapolis, MN 55455, USA

T. C. Lund · B. R. Blazar · J. Tolar
Cancer Center and the Department of Pediatrics,
Division of Hematology/Oncology,
Blood and Marrow Transplantation,
University of Minnesota, School of Medicine,
420 Delaware Street SE,
Minneapolis, MN 55455, USA

D. A. Lowe (✉)
420 Delaware St SE, MMC 388,
Minneapolis, MN 55455, USA
e-mail: lowex017@umn.edu

Introduction

Hutchinson–Gilford progeria syndrome (HGPS) is a rare and lethal childhood disease affecting approximately one in four million live births. HGPS is caused by a mutation of exon 11 in the *LMNA* gene, encoding for lamin A (De Sandre-Giovannoli et al. 2003; Eriksson et al. 2003). Lamin A is a structural protein that functions as a scaffold for the nucleus. Mutations in this protein result in structural and mechanical abnormalities of nuclei, accumulation of prelamin A (i.e., progerin) and early senescence and apoptosis of affected cells (Capell and Collins 2006; Lammerding et al. 2004). As a result, children with HGPS show symptoms of slow growth and premature aging, including alopecia, osteoporosis, vascular disease, and decreased joint mobility that are evident by the age of 3 years (Gordon et al. 2007; Hennekam 2006; Merideth et al. 2008). These children have a lifespan to mid-teenage years and commonly die of myocardial infarctions or stroke.

An incompletely understood feature of HGPS and other progeroid syndromes is that some but not all tissues are affected. Indeed, HGPS is referred to as a disease of segmental accelerated aging (Martin 1990). Halaschek-Wiener and Brooks-Wilson have nicely annotated common age-related diseases that are present and those that are absent in HGPS (Halaschek-Wiener and Brooks-Wilson 2007). The authors have proposed reasons for the presence and absence of those diseases based on the premise that tissues which require stem cells for continuous growth or repair degenerate in individuals with HGPS due to stem cell exhaustion. The age-related disease of skeletal muscle is sarcopenia and it has not been categorized as being present or absent in HGPS. Sarcopenia is characterized by muscle atrophy and weakness and is highly associated with functional impairment and immobility of the elderly (Janssen et al. 2002). Determining whether or not skeletal muscle is an affected tissue in HGPS is critical based not only on clinical importance but also on the idea that stem cells and nuclear abnormalities are fundamentally involved in the segmentation of affected tissues in HGPS.

Reasons to support the idea that skeletal muscle might not be affected in HGPS include the following. First, skeletal muscle is a post-mitotic tissue composed of multinucleated cells, collectively called muscle fibers. Thus, demands for abnormal nuclei to divide are minimal, and severely impaired nuclei could, theoretically, have compensation from neighboring nuclei to avoid apoptosis of the entire fiber. Second, part of age-induced sarcopenia is caused by denervation (Roos et al. 1997) and although peripheral neuropathy can be present in laminopathies such as Charcot–Marie–Tooth syndrome (Stewart et al. 2007), diseases of the nervous system are not common in HGPS (Halaschek-Wiener and Brooks-Wilson 2007). Third, even though muscle strength has not been documented for children with HGPS, one case study states that muscle biopsies from these children appear normal (Macnamara et al. 1970). Finally, Meredith and et al. report that "…our patients with HGPS were surprisingly active and mobile" and that muscle volume was appropriately proportioned to body size (Merideth et al. 2008). These factors are suggestive of skeletal muscle not being an affected tissue in HGPS.

Alternatively, there are also reasons to believe that skeletal muscle could be affected in HGPS. First and foremost, some mutations in the *LMNA* gene cause muscular dystrophy, for example Emery–Dreifuss and Limb–Girdle muscular dystrophies (Bonne et al. 1999; Muchir et al. 2000), with similar dystrophic pathologies evident in murine models (Grattan et al. 2005). Satellite cells, the stem-like cells in skeletal muscle that are important during growth and repair after injury, have been implicated in these muscle diseases (Frock et al. 2006). If satellite cells are affected in HGPS, the proposal of stem cell exhaustion is relevant to skeletal muscle in this disease as well. Second, it has been hypothesized that age-related muscle atrophy and weakness result from an impaired ability of muscle to repair itself following contraction-induced injuries (Faulkner et al. 1995). Here again, if HGPS satellite cells are not able to facilitate the subtle but continuous repair of muscle, premature aging would occur in a fashion similar to what is hypothesized in normal aging. Third, it has been suggested that the impaired nuclear integrity due to *LMNA* mutations are particularly problematic for tissues under high mechanical stress, such as skeletal muscle during contraction (Lammerding et al. 2004). Lastly, the case study of an HGPS patient which included analysis of a post-mortem skeletal muscle biopsy reported, "… the muscle was replaced by fibrous strands and showed wasting" (Franklyn 1976),

and a review on the musculoskeletal system of HGPS patients states that muscle atrophy is present (Hamer et al. 1988). Together these points indicate that skeletal muscle and its major function, contraction and production of force, could be detrimentally affected in HGPS.

Several mouse models have been developed to study accelerated aging. One such mouse model has a deletion of zinc metalloproteinase (*Zmpste24*) required for processing of prelamin A to lamin A. Thus, this mouse accumulates prelamin A and has many features common to HGPS (Bergo et al. 2002; Leung et al. 2001). Like HGPS, these mice have not been critically evaluated for skeletal muscle involvement. One report states that deltoid and quadriceps muscles of *Zmpste24*$^{-/-}$ mice contained abnormally small round, dystrophic fibers (Pendas et al. 2002), while another states that no fiber abnormalities could be identified in skeletal muscles throughout the limb and trunk of *Zmpste24*$^{-/-}$ mice (Bergo et al. 2002). Contractile function of skeletal muscle has not been investigated in these mice but there are indications that it might be perturbed. For example, by 8 weeks of age there is a significant inability of *Zmpste24*$^{-/-}$ mice to hang from a grid and the mice develop a slow, hobbling gait and dragging of the hindlimbs (Bergo et al. 2002).

The goal of this project was to determine the extent to which skeletal muscles of *Zmpste24*$^{-/-}$ mice were affected. We hypothesized that hindlimb muscles of *Zmpste24*$^{-/-}$ mice would display some key characteristics of age-induced sarcopenia including muscle atrophy and weakness which would be associated with decrements in physical activity and performance. Arthropathy is another common feature in progeria (Hamer et al. 1988), and if present in the *Zmpste24*$^{-/-}$ mice could contribute to poor neuromuscular performances. Therefore, we also investigated alterations in ankle joint mechanics of *Zmpste24*$^{-/-}$ mice.

Materials and methods

Animals Mice were bred from a colony at the University of Minnesota. Breeder pairs originated from the laboratory of Dr. Stephen Young (Leung et al. 2001). All mice were genotyped by PCR analysis of DNA isolated from a tail snip, with previously detailed primers (Fong et al. 2004). Mixed gender *Zmpste24*$^{+/+}$ and *Zmpste24*$^{-/-}$ mice (n=25 each) were used for this study. Mice were group housed by gender on a 12-h light–dark cycle with chow and water provided ad libitum. Body weights were recorded weekly, starting at 4 weeks of age. During the study, nine *Zmpste24*$^{-/-}$ mice died; data from these mice were not included. All protocols and animal care procedures were approved by the University of Minnesota Institutional Animal Care.

Study design Mice were assessed every 2.5 to 5 weeks for physical activity and ankle joint mechanics beginning at 5 weeks of age until 20 weeks of age. Performance via grip strength and whole body tension was assessed at 15 or 20 weeks of age. Also at 15 or 20 weeks of age, soleus and extensor digitorum longus (EDL) muscles were dissected and analyzed ex vivo for contractile functions. A subset of 20-week-old mice also underwent in vivo contractile testing of the left leg. Following the contractility analyses, hindlimb muscles and strips of diaphragm muscle were weighed, snap frozen in liquid nitrogen, and stored at −80°C or were frozen in optimal cutting temperature medium for histological analyses. While still under anesthesia, mice were euthanized by exsanguination.

Physical activity Twenty-four-hour cage activity was assessed using open field activity chambers (Med Associates Inc., St. Albans, VT) (Greising et al. 2011). Briefly, chambers contain infrared arrays in the *x*-, *y*-, and *z*-axes with two sets of beams in the *x*-direction, one being elevated to 2.5 or 5.4 cm above the bottom of the cage for *Zmpste24*$^{-/-}$ and *Zmpste24*$^{+/+}$ mice, respectively (to account for their body size differences). Activity Monitor version 6.01 software was used to collect data with a box size set to "2" (3.2 cm^2) which is used to calculate movement, delay, and filter the data. Activity measurements included distance traveled, jumping, rearing and stereotypic counts, and total active time during a 24-h period.

Performance testing Performance was assessed via grip strength and whole body tension (Call et al. 2010). For each trial of grip strength, mice grasped a bar that was attached to a force transducer (Grip Strength Meter; Columbus Instruments, Columbus, OH). For whole body tension, mice were attached to a force transducer (BIOPAC Systems, Inc., Goleta, CA)

by suture attached to their tail and were then induced to move forward by tail pinches over a 90-s period. Performance was calculated for each test by averaging the top 5 peak forces recorded. Both tests were conducted by the same investigator and data are reported as force normalized to body mass.

Ankle joint mechanics Mice were anesthetized with a cocktail of fentanyl citrate (10 mg/kg), droperidol (0.2 mg/kg), and diazepam (5 mg/kg). Passive torque about the left ankle joint was assessed by stabilizing the knee and placing the foot in a plate attached to a servomotor (300B-LR, Aurora Scientific, Aurora, Ontario, Canada) (Baltgalvis et al. 2009; Garlich et al. 2010). The servomotor rotated the ankle to four angles of dorsiflexion (5°, 10°, 15°, and 20°) and four angles of plantarflexion (5°, 10°, 15°, and 20°) and torque was measured at each angle. Range of motion (ROM) about the left ankle joint was measured while the mouse was stabilized in a position in which the hip and knee were both at 90° of flexion (Garlich et al. 2010). The ankle joint was moved into end-range dorsi- and plantarflexion, and images were acquired at those positions and then analyzed using ImageJ software (Frederick, MD) (Garlich et al. 2010).

Skeletal muscle contractility in vivo At 20 weeks of age, immediately following testing of joint mechanics and while still anesthetized, mice underwent in vivo contractile testing of the left leg (Baltgalvis et al. 2009; Garlich et al. 2010). First, maximal isometric torque of the anterior leg muscle group was measured by subdermal stimulation of the common peroneal nerve. Second, maximal isometric torque of the posterior leg muscle group (soleus, plantaris, and gastrocnemius muscles) was measured by stimulation of the sciatic nerve, with the common peroneal nerve severed. Stimulation was 200-ms total duration consisting of 0.5-ms square-wave pulses at 300 Hz (models S48 and SIU5, respectively, Grass Technologies, West Warwick, RI). The voltage was adjusted from 3.0 to 9.0 V until maximal isometric torques were achieved on the 300B-LR servomotor.

Skeletal muscle contractility ex vivo A subset of mice at 15 and 20 weeks of age underwent testing of isolated soleus and EDL muscles (Moran et al. 2005; Moran et al. 2006). Contractile characteristics tested included; peak twitch force (P_t), time to peak twitch, one half twitch relaxation time (1/2 RT), maximal isometric tetanic force (P_o), rates of force development and relaxation ($+dP/dt$ and $-dP/dt$), and active and passive stiffness.

Serum creatine kinase activity Blood was collected from anesthetized mice at 20 weeks of age from the retrooribital sinus. Blood was allowed to clot and serum was separated and stored at −80°C until analysis. Creatine kinase activity was analyzed on Vitros CK/CPK slides (Ortho Clinical Vitros DT60 II Dry Slides) and run on a spectrophotometer (Ortho Clinical Vitros DT II System). Creatine kinase activity is reported as units/liter (U/L).

Histo-morphological analyses Serial sections from the mid-belly of muscles frozen in OCT compound were cut to 10-μm thickness. Cross-sectional area of ~200 fibers per soleus, and EDL muscle were measured from hematoxylin and eosin-stained sections (Landisch et al. 2008). Capillarity of those muscles were assessed by the periodic acid-Schiff reaction (Josephson 1993). The next three sections of each muscle were analyzed for fiber type via myosin heavy chain isoform I, IIa, or IIb (Landisch et al. 2008). If a fiber did not react to either the myosin heavy chain I, IIa, or IIb antibody, it was classified as a IIx fiber. The final serial sections were used to assess the abundance of nuclei in relationship to the ~200 fibers analyzed. For this, nuclei were labeled using DAPI and a dystrophin antibody (1:20 dilution of NCL-DYS1; Novocastra Laboratories, Newcastle upon Tyne) was used to define the sarcolemma; nuclei were counted as myonuclei per fiber, central nuclei per fiber, or extracellular-related nuclei per total area (Landisch et al. 2008; Moran et al. 2005). Care was taken not to count nuclei if they appeared to be in a vessel. A single investigator who was blinded to genotype conducted each type of histological analysis. Additional 6-μm EDL and soleus muscle sections were examined for the localization of emerin at the nuclear rim using antibodies for emerin (1:25 dilution of ab14208; Abcam, Cambridge MA), dystrophin (1:20 dilution of NCL-DYS1; Novocastra Laboratories, Newcastle upon Tyne), and DAPI.

Hydroxyproline content of frozen EDL, tibialis anterior, soleus, and gastrocnemius muscles were measured biochemically to asses total collagen content (Garlich et al. 2010; Reddy and Enwemeka 1996). Western blot analyses for lamin A/C and

prelamin A were carried out on EDL and soleus muscles to assess accumulation of prelamin A. Each frozen muscle was homogenized on ice in 25 mM Tris HCL, 150 mM NaCl, 1% igepal CA-630, 1% sodium deoxycholate, and 0.1% SDS; 5 μL of benzonase nuclease was added to each sample. Approximately, 0.5 μg of protein from each sample was loaded on a 4–12% Bis-Tris gel. Following electrophoresis, proteins were transferred to nitrocellulose membranes and probed using 1:500 dilutions of a Lamin A/C antibody (sc-6215; Santa Cruz Biotechnology, Inc., Santa Cruz, CA) and Histone H3 antibody (ab61251; Abcam, Cambridge, MA). Blots were analyzed for the ratio of prelamin A to histone H3 and comparisons made between EDL and soleus muscles of *Zmpste24*$^{-/-}$ mice.

Statistical analysis *Zmpste24*$^{+/+}$ mice at 15 and 20 weeks of age were not significantly different as determined by Student's *t* tests ($p \geq 0.088$) on any measured parameter and therefore these data were collapsed to represent a single control group. Likewise, *Zmpste24*$^{-/-}$ mice were not significantly different at 15 and 20 weeks of age ($p \geq 0.087$), and these data were collapsed. Data were analyzed by Student's *t* test to determine differences between genotypes for in vivo joint mechanics, and ex vivo contractility measurements, creatine kinase activity, muscle masses, collagen content, and histological analyses. A Student's *t* test was also used to compare prelamin A accumulation between EDL and soleus muscles. Chi-square tests were used to analyze the frequency distribution of EDL and soleus muscle fiber cross-sectional area. Longitudinal data were analyzed by two-way repeated measures ANOVA to determine differences between genotypes over time for body mass, physical activity, ROM, and passive torque. Statistical analyses were conducted using SigmaStat version 3.5 (Systat Software Inc; Point Richmond, CA). Significance was accepted at the $\alpha < 0.05$ level. Data are presented as mean±standard error.

Results

Body mass and neuromuscular performance

Body mass *Zmpste24*$^{-/-}$ mice had halted growth by 5 weeks of age and had lower body mass relative to *Zmpste24*$^{+/+}$ littermates through 20 weeks of age. At 20 weeks of age, the difference in body mass between *Zmpste24*$^{-/-}$ and *Zmpste24*$^{+/+}$ littermates was >50% (12.9±0.7 g vs. 28.1±1.2 g; $p < 0.001$).

Physical activity *Zmpste24*$^{-/-}$ mice were less active than were their *Zmpste24*$^{+/+}$ littermates ($p < 0.001$; Fig. 1). Over the 15-week study period, *Zmpste24*$^{-/-}$ mice averaged 53% less distance traveled and spent ~37% less time being active, the latter equating to almost a 2-h difference per day. Jumping and stereotypic activities were also ~70% less in the *Zmpste24*$^{-/-}$ mice ($p \leq 0.011$). There was no difference in hindlimb rearing between the groups ($p = 0.231$).

Grip strength and whole body tension Grip strength was impaired in the *Zmpste24*$^{-/-}$ mice (2.4±0.4 g/g body mass vs. 3.6±0.3 g/g for *Zmpste24*$^{+/+}$ littermates; $p = 0.038$). Notably, most *Zmpste24*$^{-/-}$ mice had difficulty grasping the bar to perform the grip strength test which likely confounded these results. Whole body tension, corrected for the smaller size of

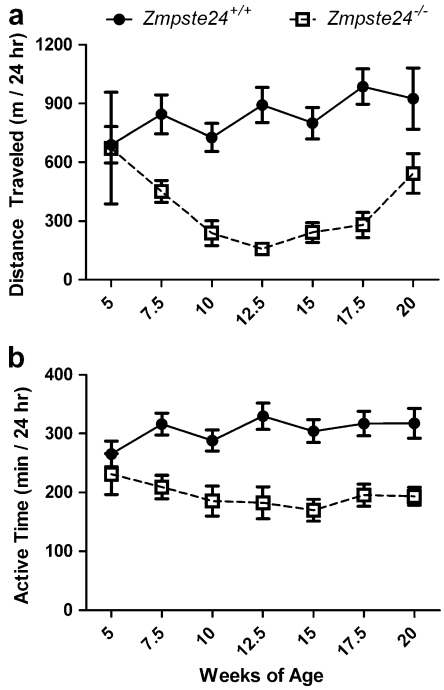

Fig. 1 Daily cage activities of *Zmpste24*$^{+/+}$ and *Zmpste24*$^{-/-}$ mice from 5 to 20 weeks of age. **a** Ambulation distance traveled in the cage per 24 h. **b** Time spent being active in the cage per 24 h. Data are presented as means±SE; $n = 3$ to 13 per genotype per time point

Zmpste24$^{-/-}$ mice, showed a trend for these mice to have poor performance as *Zmpste24*$^{-/-}$ mice pulled 7.3±0.9 g/g body mass vs. 9.9±1.0 g/g for *Zmpste24*$^{+/+}$ mice (p=0.056).

Ankle joint mechanics

Range of motion Ankle joint ROM changed with age, and did so differently between *Zmpste24*$^{-/-}$ and *Zmpste24*$^{+/+}$ mice for both dorsi- and plantarflexion (interactions p<0.001). At each age tested, *Zmpste24*$^{-/-}$ mice had 20–70% less dorsi- and plantarflexion than *Zmpste24*$^{+/+}$ littermates (Fig. 2). *Zmpste24*$^{-/-}$ mice had progressively decreasing dorsiflexion ROM as they aged, with those at 10, 15, and 20 weeks being less than at 5 weeks of age (Fig. 2). Plantarflexion ROM also decreased with age in the *Zmpste24*$^{-/-}$ mice, as opposed to a slight increase with age in the *Zmpste24*$^{+/+}$ mice. Overall, at 20 weeks of age, *Zmpste24*$^{-/-}$ mice were functioning with 71% less ROM about the ankle than were *Zmpste24*$^{+/+}$ littermates (44±4^{o} vs. 150±2^{o}; p<0.001).

Passive torque Passive torque about the ankle represents the force applied to the foot that is required to rotate the ankle when the lower limb muscles are inactive. Differences at some degrees of dorsi- and plantarflexion were significant between *Zmpste24*$^{-/-}$ and *Zmpste24*$^{+/+}$ mice at the ages of 5, 10, and 15 weeks (data not shown), but the greatest differences were detected at 20 weeks of age at which time *Zmpste24*$^{-/-}$ mice had greater passive torques at 10, 15, and 20^{o} of both plantar- and dorsiflexion compared with *Zmpste24*$^{+/+}$ littermates (p≤0.004; Fig. 3). These exceptionally high passive torques, particularly those required to move the foot into dorsiflexion, exemplify a stiff joint.

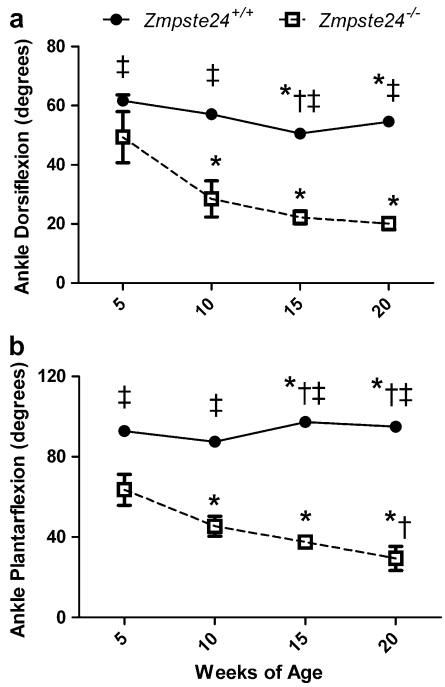

Fig. 2 Range of motion about the ankle joint in *Zmpste24*$^{+/+}$ and *Zmpste24*$^{-/-}$ mice from 5 to 20 weeks of age. Data are presented as means±SE; n=3 to 13 per genotype per time point. For many data points, the *error bars* are within the *symbols* representing the means. *Asterisk*, within genotype, significantly different than 5 weeks of age. *Dagger*, within genotype, significantly different than 10 weeks of age. *Double dagger*, significantly different than *Zmpste24*$^{-/-}$ mice at corresponding age

Skeletal muscle contractility

In vivo muscle strength The posterior leg muscles (soleus, plantaris, and gastrocnemius muscles) of *Zmpste24*$^{-/-}$ mice were weaker than those of *Zmpste24*$^{+/+}$ mice (p<0.001; Fig. 4a, left; 6.6±0.7 vs. 14.6±0.5 N·mm of torque, respectively). However, when torque was normalized to the small posterior muscle masses of the *Zmpste24*$^{-/-}$ mice, strength was not lower than that of *Zmpste24*$^{+/+}$ mice (122.7±4.5 vs. 104.3±3.3 kN·mm^{-1} kg^{-1} muscle, respectively; p=0.091).

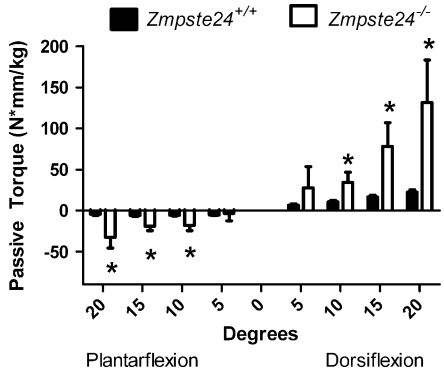

Fig. 3 Passive torque about the ankle joint in *Zmpste24*$^{+/+}$ and *Zmpste24*$^{-/-}$ mice aged 20 weeks. Data are normalized to body mass and presented as means±SE; n=3 to 13 per genotype

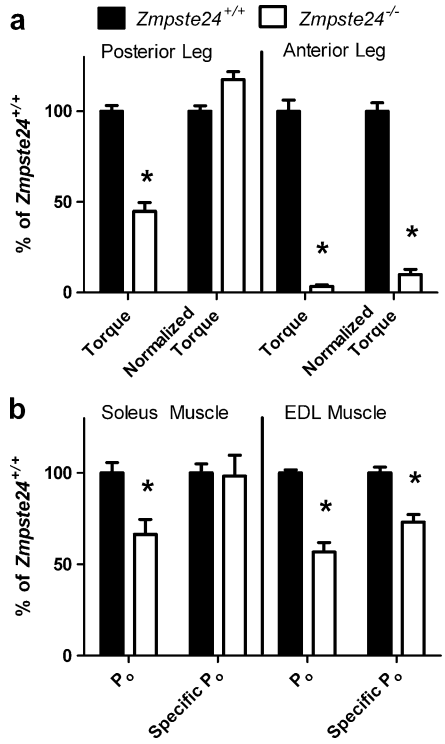

Fig. 4 Force-generating capacities of leg muscles from *Zmpste24*$^{+/+}$and *Zmpste24*$^{-/-}$ mice from 15 to 20 weeks of age. **a** Maximal isometric torque of muscle groups of the leg. **b** Maximal isometric force (P_o) of isolated leg muscles. Normalized torque is maximal torque relative to the sum of respective muscle masses. Specific P_o is maximal isometric tetanic force relative to physiological cross-sectional area of the muscle. Data are shown relative to *Zmpste24*$^{+/+}$mice and presented as means±SE; n=3 to 14 per genotype. *Asterisk*, significantly different than *Zmpste24*$^{+/+}$mice

Strength of the anterior leg muscles (extensor hallucis longus, EDL and tibialis anterior muscles) of *Zmpste24*$^{-/-}$ mice was more severely affected than was strength of the posterior leg muscles (Fig. 4a, right). Maximal torque production of the anterior leg muscles of *Zmpste24*$^{-/-}$ mice averaged 0.1±0.02 vs. 6.5±0.2 N·mm for *Zmpste24*$^{+/+}$ mice (p<0.001). This difference could not be explained by smaller muscles because torque normalized to the mass of the anterior muscles was still extremely low in the *Zmpste24*$^{-/-}$ mice (5.0±1.5 vs. 50.5±2.3 kN·mm^{-1} kg^{-1} muscle for *Zmpste24*$^{+/+}$ mice; p<0.001).

Ex vivo muscle strength The absolute maximal P_o generated by isolated soleus muscles from *Zmpste24*$^{-/-}$ mice was 34% less than that from than *Zmpste24*$^{+/+}$ littermates (109.7±13.4 vs. 165.4±9.4 mN, respectively; p=0.002; Fig. 4b, left). However, when normalized to cross-sectional area of the muscles (specific P_o) there was no difference between groups with an overall average 13.0±0.7 N/cm^2 of force (p=0.879; Fig. 4). On the contrary, both P_o and specific P_o of EDL muscles were ~40% lower in *Zmpste24*$^{-/-}$ than *Zmpste24*$^{+/+}$ mice (p<0.001; Fig. 4b, right; 203.6±18.7 vs. 359.1±6.1 mN and 14.4±0.9 vs. 19.8±0.6 N/cm^2, respectively). These results follow the same pattern as the in vivo strength analyses, that is, the muscles on the anterior leg (tibialis anterior and EDL muscles) were much more severely affected than were the opposing posterior leg muscles (gastrocnemius and soleus muscles).

Additional contractile characteristics of soleus and EDL muscles further demonstrated the impact of accelerated aging on skeletal muscle. Peak twitch force and active stiffness are parameters related to force generation and EDL but not soleus muscles from the *Zmpste24*$^{-/-}$ mice showed weakness (Table 1), consistent with the P_o results. The muscles' ability to relax after contraction was consistently diminished in *Zmpste24*$^{-/-}$ mice as indicated by longer twitch one-

Table 1 Ex vivo contractile properties of soleus and EDL muscles of *Zmpste24*$^{+/+}$ and *Zmpste24*$^{-/-}$ mice

	Zmpste24$^{+/+}$	*Zmpste24*$^{-/-}$	p value
Soleus muscle (n)	(13)	(10)	
P_t (mN)	26.4±1.5	24.7±2.7	0.507
TPT (ms)	35.0±1.0	43.1±3.8	0.026
1/2 RT (ms)	4.0±0.1	5.7±0.8	0.022
+dP/dt (N/s)	1.7±0.1	1.5±0.2	0.510
−dP/dt (N/s)	3.3±0.3	1.6±0.2	0.002
Active stiffness (N/m)	269.3±15.1	241.6±22.7	0.301
Passive stiffness (N/m)	11.5±0.4	16.5±1.4	<0.001
EDL muscle (n)	(11)	(11)	
P_t (mN)	69.5±2.1	35.4±2.6	<0.001
TPT (ms)	19.3±0.3	18.2±1.5	0.475
1/2 RT (ms)	1.8±0.1	2.2±0.1	<0.001
+dP/dt (N/s)	7.3±0.2	4.2±0.4	<0.001
−dP/dt (N/s)	21.4±0.5	7.9±1.3	<0.001
Active stiffness (N/m)	433.6±14.2	299.3±22.2	<0.001
Passive stiffness (N/m)	12.2±0.5	18.2±1.0	<0.001

Mean±SE

P_t peak twitch force, *TPT* time to peak twitch force, *1/2 RT* one half relaxation time, *+dP/dt* maximal rate of tectanic force development, *−dP/dt* maximal rate of relaxation

half relaxation times and slower tetanic rates of relaxation in both soleus and EDL muscles relative to those of *Zmpste24*$^{+/+}$ mice (Table 1). Passive stiffness, indicative of muscles' elastic properties and resistance to lengthening while not contracting, was also high in both soleus and EDL muscles of *Zmpste24*$^{-/-}$ mice.

Serum creatine kinase activity

Creatine kinase in the serum is a common marker of skeletal muscle injury and high creatine kinase values are regularly used as a diagnostic tool for muscular dystrophies. There was not a significant difference in serum creatine kinase activity between 20-week-old *Zmpste24*$^{-/-}$ and *Zmpste24*$^{+/+}$ littermates (3,404±761 vs. 2,003±415 UL, respectively; p=0.150).

Skeletal muscle histo-morphometry

Muscle masses All leg muscles of *Zmpste24*$^{-/-}$ mice were smaller than those of *Zmpste24*$^{+/+}$ littermates, weighing on average 42% less (p<0.001). When the substantial difference in body masses were accounted for by normalizing muscle mass to body mass, the tibialis anterior, soleus, and gastrocnemius muscles were not different between groups (Table 2). EDL muscle to body mass was relatively greater in *Zmpste24*$^{-/-}$ mice (Table 2).

Collagen content Collagen content of the leg muscles was measured because passive stiffness of both EDL and soleus muscles was high in *Zmpste24*$^{-/-}$ mice. Total collagen content of the EDL, tibialis anterior, soleus, and gastrocnemius muscles was 45–72% greater in *Zmpste24*$^{-/-}$ compared with *Zmpste24*$^{+/+}$ mice (Table 2).

Prelamin A content The content of prelamin A was measured in soleus and EDL muscles to determine if the contractile differences between those muscles in the *Zmpste24*$^{-/-}$ mice were associated with the accumulation of prelamin A (Fig. 5). There was no difference in the ratio of prelamin A to histone H3 between soleus and EDL muscles of *Zmpste24*$^{-/-}$ mice (0.85±0.2 vs. 0.91±0.1, respectively; p=0.804).

Histological characteristics of soleus muscles The mean cross-sectional area of all soleus muscle fibers was not different between *Zmpste24*$^{-/-}$ and *Zmpste24*$^{+/+}$ mice (1,431±74 vs. 1,418±156 μm^2, respectively; p=0.946). Despite this, there was a significantly different distribution of fiber sizes with soleus muscles from *Zmpste24*$^{-/-}$ mice having a broadened distribution with more small and large fibers compared with those of *Zmpste24*$^{+/+}$ littermates (p<0.001; Fig. 6a). Soleus muscles from *Zmpste24*$^{-/-}$ mice contained the same percentages of myosin heavy chain type I, IIa, and IIx fibers as those from *Zmpste24*$^{+/+}$ littermates (Table 3). Capillarity of soleus muscle was not affected by the lack of *Zmpste24* (Table 3). Muscles were analyzed for nuclear content because on initial observations of hematoxylin and eosin-stained sections, there were noticeably more nuclei (e.g., Fig. 7). There were no differences between *Zmpste24*$^{-/-}$ and *Zmpste24*$^{+/+}$ mice in the percent of soleus muscle fibers with centrally located nuclei or nuclei in the extracellular space, but there were significantly more myonuclei in soleus muscles of *Zmpste24*$^{-/-}$ mice. Other than the

Table 2 Masses and content of leg muscles of *Zmpste24*$^{+/+}$ and *Zmpste24*$^{-/-}$ mice

	Zmpste24$^{+/+}$	*Zmpste24*$^{-/-}$	p value
Muscle mass (mg/g) (n)	(25)	(16)	
Extensor digitorum longus	0.38±0.02	0.47±0.02	0.003
Tibialis anterior	1.74±0.09	1.82±0.13	0.588
Soleus	0.33±0.03	0.36±0.01	0.322
Gastrocnemius	5.25±0.28	5.15±0.13	0.772
Collagen content (μg/mg) (n)	(8–13)	(3–13)	
Extensor digitorum longus	10.7±2.3	17.2±2.0	0.005
Tibialis anterior	17.4±0.5	27.4±2.5	<0.001
Soleus	17.8±3.2	30.6±2.5	<0.001
Gastrocnemius	19.2±2.3	27.8±1.2	<0.001

Mean±SE. Muscle masses normalized to body mass. Collagen contents normalized to muscle masses

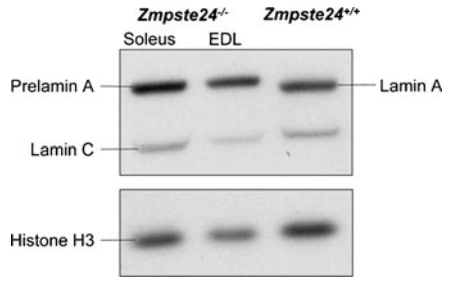

Fig. 5 Representative blots of prelamin A expression (~73 kDa), relative to histone H3 (15 kDa), in soleus and EDL muscles of *Zmpste24*$^{-/-}$ mice. Prelamin A is only distinguishable in the *Zmpste24*$^{-/-}$ muscles, while *Zmpste24*$^{+/+}$ muscles have lamin A (69 kDa) and lamin C (62 kDa). The complete analysis was conducted on 12 independent samples; six soleus and six EDL muscles, half from *Zmpste24*$^{-/-}$ and half from *Zmpste24*$^{+/+}$ mice

abundance of myonuclei, there were no other obvious signs of histopathology in soleus muscles of these mice (Fig. 7).

Histological characteristics of EDL muscles Relative to the minor histological differences between soleus muscles of *Zmpste24*$^{-/-}$ and *Zmpste24*$^{+/+}$ mice, EDL muscles were slightly more affected. EDL muscle fibers of *Zmpste24*$^{-/-}$ mice were small relative to those of littermates as illustrated by the significant leftward shift in the distribution of fiber cross-sectional areas ($p<0.001$; Fig. 6b) and a trend for the overall mean fiber cross-sectional area to be less (837±38 vs. 1,004±99 μm^2 for *Zmpste24*$^{-/-}$ and *Zmpste24*$^{+/+}$ mice, respectively; $p=0.071$). There was a difference in fiber-type composition in EDL muscles with those from *Zmpste24*$^{-/-}$ mice having relatively more Type IIa and less Type IIb fibers (Table 3), indicating a fiber-type shift toward a myosin heavy chain isoform that is typically associated with fast-twitch kinetics and both oxidative and glycolytic energetics. Similar to soleus muscles, there were no differences between mice in EDL muscle capillarity, central nuclei, or nuclei in the extracellular space, but EDL muscle fibers of *Zmpste24*$^{-/-}$ mice contained significantly more myonuclei than those of *Zmpste24*$^{+/+}$ mice (Table 3). Aside from the myonuclei, no other histological differences were observed (Fig. 7).

Additional histological characteristics Tibialis anterior, gastrocnemius, quadriceps, and diaphragm muscles from a subset of mice were subjectively evaluated using H&E staining. Soleus and EDL muscles were also evaluated for the localization of emerin to the nuclear rim. All muscles of *Zmpste24*$^{-/-}$ mice that were evaluated appeared normal and healthy. For example, there were no signs of dystrophic features such as central nuclei, degenerating fibers, fibrosis, or mislocalization of emerin (see Figs. 7 and 8). Both *Zmpste24*$^{-/-}$ and *Zmpste24*$^{+/+}$ mice had emerin present at the nuclei (Fig. 8).

Discussion

Using a variety of tests for assessing the function of skeletal muscle, we show that *Zmpste24*$^{-/-}$ mice have impaired neuromuscular performance and selective muscle weakness relative to their *Zmpste24*$^{+/+}$ litter-

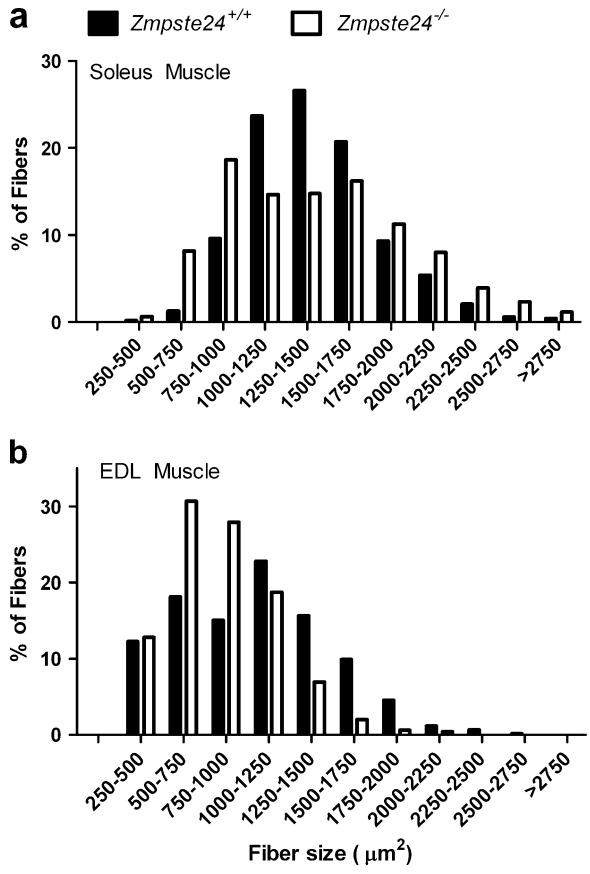

Fig. 6 Fiber cross-sectional area distribution of soleus (**a**) and EDL (**b**) muscles from *Zmpste24*$^{+/+}$ and *Zmpste24*$^{-/-}$ mice aged 20 weeks. Data are presented as means; $n=4$ to 6 per genotype per muscle

Table 3 Histological characteristics of soleus and EDL muscles of *Zmpste24*$^{+/+}$ and *Zmpste24*$^{-/-}$ mice

	Zmpste24$^{+/+}$	*Zmpste24*$^{-/-}$	*p* value
Soleus muscle (*n*)	(5)	(5)	
% Type I	38.3±2.6	33.7±2.1	0.203
% Type IIa	59.3±3.0	63.4±2.0	0.277
% Type IIx	2.2±0.6	3.1±1.4	0.559
Capillaries per fiber	3.3±0.1	3.4±0.1	0.775
% Central nuclei	0.72±0.4	0.76±0.5	0.961
Myonuclei per fiber	2.7±0.2	3.3±0.2	0.023
Extracellular nuclei per area (mm^2)	2.1±0.5	2.1±0.4	0.889
EDL muscle (*n*)	(4)	(5)	
% Type I	2.0±0.5	4.1±0.8	0.079
% Type IIa	12.3±1.8	22.2±1.8	0.007
% Type IIx	23.0±2.2	25.8±2.8	0.467
% Type IIb	62.5±3.3	48.0±2.9	0.013
Capillaries per fiber	2.2±0.3	2.2±0.2	0.683
% Central nuclei	1.3±0.2	2.3±0.4	0.078
Myonuclei per fiber	1.9±0.2	2.4±0.1	0.004
Extracellular nuclei per area (mm^2)	4.7±2.1	6.2±3.2	0.511

Mean±SE. Fiber types based on myosin heavy chain immunohistochemistry and expressed as percentages of total number of fibers. No soleus muscle fibers expressed myosin heavy chain IIb.% Central nuclei, percent of fibers that had central nuclei

mates. These physiological characteristics are similar to those of aged mice and indicate that some characteristics of sarcopenia are present in this progeroid mouse model. In mice that are aged normally and in the *Zmpste24*$^{-/-}$ mouse model of accelerated aging, force generation as well as rates of muscle contraction are impaired (Brooks and Faulkner 1988; Moran et al. 2005), as are parameters of neuromuscular performance (Carlson et al. 2010; Ingram 2000). Collectively, these results suggest that skeletal muscle is an affected tissue in HGPS.

This is the first report of perturbations in skeletal muscle contractility in a mouse model of HGPS. Because the primary function of skeletal muscle is to contract and generate force, direct measures of contractility are required to substantiate the involvement of skeletal muscle in progeria. We found that force generation by leg muscles was 30–95% lower in 15- and 20-week-old *Zmpste24*$^{-/-}$ than *Zmpste24*$^{+/+}$ mice indicating a general muscle weakness. The weakness exhibited by isolated soleus muscle and the posterior leg muscles in vivo were completely explained by the small size of those muscles, which in turn were proportional to the small size of the mice. A similar situation appears to exist in HGPS patients as proportional scaling of skeletal muscle to body size has been reported (Gordon et al. 2007; Hamer et al. 1988; Merideth et al. 2008).

In contrast, muscle size could not account for the exceptionally low contractile capacities of isolated EDL muscle and of the anterior leg muscles in vivo. All skeletal muscles that were assessed for prelamin A showed that the protein was present in those from *Zmpste24*$^{-/-}$ mice and not from *Zmpste24*$^{+/+}$ mice, but accumulation of prelamin A was similar between EDL and soleus muscles and, thus, could not explain why anterior but not posterior leg muscles were weak. Bergo et al. described a severe effacement of the anterior tibial tuberosity, the origin of the tibialis anterior muscle, in *Zmpste24*$^{-/-}$ mice and suggested that lower extremity weakness contributed to the bone abnormality (Bergo et al. 2002). It is conceivable that the reverse situation occurs, that is, the tibial bone effacement contributes to anterior leg muscle weakness because the tibialis anterior muscle, the largest of the anterior leg muscles, is not able to transmit force to the bone properly. *Zmpste24*$^{-/-}$ mice exhibit tibial bone loss as a result of low osteoblasts and osteoclasts relative to bone volume (Rivas et al. 2009). Likewise, bone abnormalities are a common feature in HGPS (Gordon et al. 2007; Hamer et al. 1988; Merideth et al. 2008).

An alternative possibility is that muscle and bone abnormalities co-evolve during the development of progeria. In addition to the selective contractile deficits we detected, we also noted several anatomical

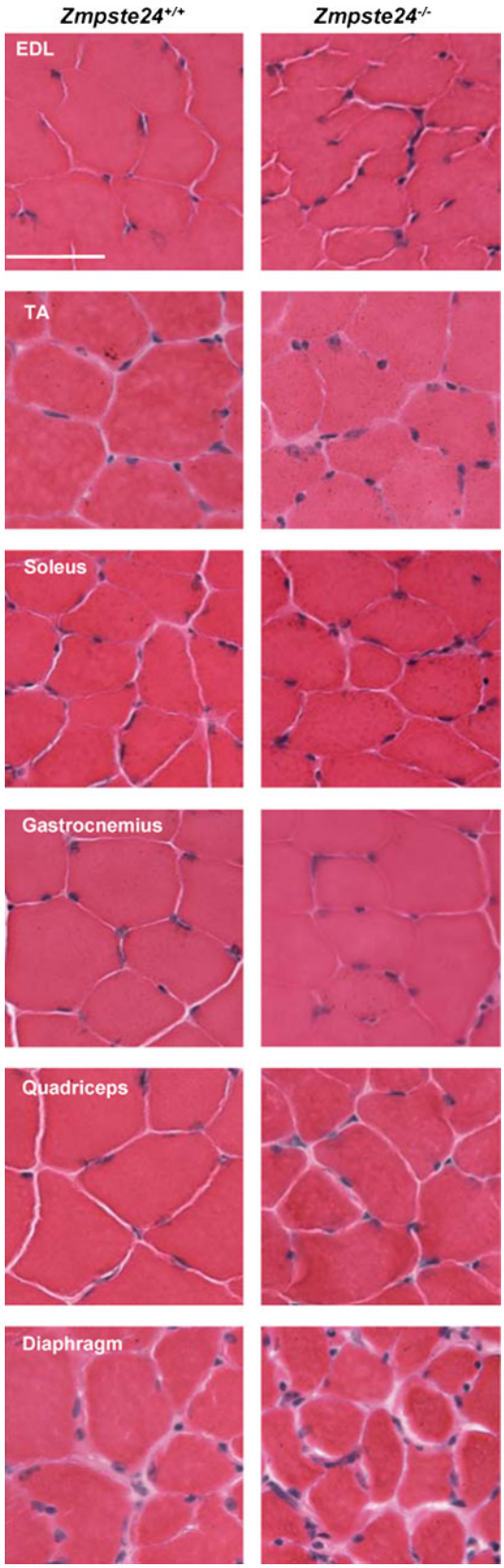

Fig. 7 Representative cross-sections of hematoxylin and eosin-stained EDL, tibialis anterior (*TA*), soleus, gastrocnemius, quadriceps, and diaphragm muscles from *Zmpste24*$^{+/+}$and *Zmpste24*$^{-/-}$ mice. *Scale bar* is 50 μm

abnormalities in the leg musculature of *Zmpste24*$^{-/-}$ mice. In four of these mice, either the EDL or soleus muscle was partially fused with an adjacent muscle (in which cases those muscles were not assessed for contractility). Two *Zmpste24*$^{-/-}$ mice had EDL muscles that were abnormally deep within the anterior leg compartment, and another mouse did not have distinguishable heads of the gastrocnemius muscle. We speculate that the pathologies found in bone and now in skeletal muscle may co-exist due to these tissues' common mesenchymal origin. Evidence for the involvement of stem cells in physiological aging and accelerated aging diseases is mounting, particularly for mesenchymal stem cells (Pekovic and Hutchison 2008). For example, Scaffidi and Misteli showed that progerin interfered with the differentiation of mesenchymal stem cells toward fat, bone, and cartilage (Scaffidi and Misteli 2008). The other cellular component important in muscle growth and development is that of satellite cells, and although myogenesis was not investigated in the study by Scaffidi and Misteli, other studies have shown that satellite cell and myoblast differentiation are impacted by prelamin A and lamin A perturbations (Frock et al. 2006; Maraldi et al. 2011). Additional in vivo studies on myogenesis and satellite cell function in *Zmpste24*$^{-/-}$ mice are needed to substantiate speculations on the involvement of mesenchymal stem cells in HGPS. These types of investigations are also critical to elucidate the involvement of unprocessed lamin A in physiological muscle injury and regeneration.

Despite the anatomical leg muscle abnormalities noted, minimal histopathological manifestations were observed in skeletal muscles of *Zmpste24*$^{-/-}$ mice. This is in agreement with Bergo et al. who stated that no histological abnormalities of skeletal muscle in these mice could be identified (Bergo et al. 2002), and contrary to another group who reported that *Zmpste24*$^{-/-}$ mice had dystrophic fibers (Pendas et al. 2002). Our histological evaluations of hindlimb and diaphragm muscles from 15- and 20-week-old *Zmpste24*$^{-/-}$ mice did not reveal primary indications of muscular dystrophy such as inflammation, fibrosis, necrosis, fibers with centralized nuclei, or mis-

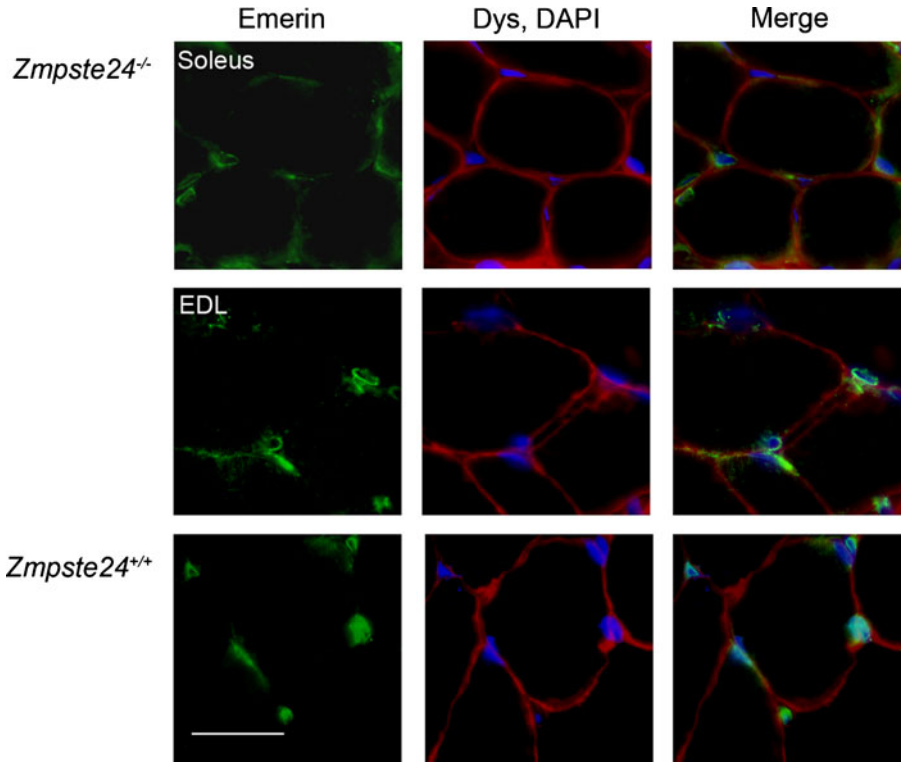

Fig. 8 Representative cross-sections of immunofluorescently stained EDL and soleus muscles from *Zmpste24*$^{+/+}$and *Zmpste24*$^{-/-}$ mice. Muscles were stained with antibodies against emerin (*green*), dystrophin (*Dys*, *red*), and DAPI (*blue*). *Scale bar* is 25 μm

localization of emerin at the nuclear rim (Sullivan et al. 1999) (nor elevated serum creatine kinase activity (Emery 2002)). The only histological aberration that we consistently observed was excessive myonuclei in fibers of *Zmpste24*$^{-/-}$ mice. The cause and consequence of these extra myonuclei are not known but theoretically could relate to nuclear pathology or shortened telomeres that have been associated with progeria (Capell and Collins 2006; Rodriguez and Eriksson 2010). The soleus and EDL muscles in which excessive nuclei were found were from the same *Zmpste24*$^{-/-}$ mice assessed for contractile function, but because nuclei per se are not involved in the generation of force it is difficult to speculate how excessive nuclei could directly cause muscle weakness.

Fibrosis or fat accumulation were not obvious from the histological evaluations of muscle cross-sections from *Zmpste24*$^{-/-}$ mice. Increased fat mass sometimes occurs with sarcopenia (Fielding et al. 2011) and is an additional parameter that should be assessed in the muscles of *Zmpste24*$^{-/-}$ mice in the future. Instead, in this study we chose to assess muscle collagen content because of the high passive stiffness measured in soleus and EDL muscles from *Zmpste24*$^{-/-}$ mice. These biochemical analyses revealed that total collagen content of all four skeletal muscles assayed was quite high relative to that of muscles from *Zmpste24*$^{+/+}$ mice. The surplus of collagen was likely the cause of the high passive stiffness. Similar connective tissue accumulation in heart and vascular smooth muscle cells have been shown in progeria mouse models (Pendas et al. 2002; Varga et al. 2006), as well as in HGPS (Olive et al. 2010), but this is the first report in skeletal muscle. Collectively, these results provide evidence for a connective tissue involvement in muscle (skeletal, smooth, and cardiac) in premature accelerated aging, perhaps indicating prior inflammation in these tissues.

Connective tissue involvement is evident in other age-related diseases in HGPS including alopecia, nail defects, sclerotic skin, dental malformations, and osteoporosis (Halaschek-Wiener and Brooks-Wilson 2007; Merideth et al. 2008). Arthropathy such as joint stiffness is also a common feature of HGPS (Gordon et al. 2007; Merideth et al. 2008), but had not previously been investigated in progeria mouse models. In preliminary investigations on anesthetized *Zmpste24*$^{-/-}$ mice, it was quite apparent that wrist, ankle, knee, and hip joints were very resistant to

movement. This prompted us to quantitate joint mechanics and we selected to evaluate the ankle because it is the joint associated with the skeletal muscles analyzed. We found that the torque required to move the ankle into dorsi- and plantarflexion increased as the *Zmpste24*$^{-/-}$ mice aged, and in parallel, ROM about the ankle progressively decline from 5 to 20 weeks of age while those of littermates remained constant. Abnormal joint mobility has been reported in HGPS patients with ROM deficiencies of similar magnitude, 58 and 49% decrements in wrist and ankle ROMs, respectively (Merideth et al. 2008), to what we observed in the ankle of *Zmpste24*$^{-/-}$ mice. It is reasonable to conjecture that these joint problems contributed to the slow gait and hindlimb dragging reported previously (Bergo et al. 2002) and to the reduced cage activities measured in this study. Furthermore, the ability of *Zmpste24*$^{-/-}$ mice to grasp the bar for the grip strength measurement was clearly impaired in this study and likely contributed to the low grip strength and possibly to the report of reduced hang time (Bergo et al. 2002). It is probable that this arthropathy contributed to reduced physical activity by *Zmpste24*$^{-/-}$ mice. Disuse is one of the underlying causes of sarcopenia (Fielding et al. 2011) and is likely associated with muscle weakness in these progeria mice as well. In a preliminary study, we attempted to overcome disuse by providing *Zmpste24*$^{-/-}$ mice running wheels in their cages. The mice ran 1–3 km per 24 h for ~75 days but then running dramatically dropped off and mice stopped running. We speculate that the arthropathy became so severe that mice were not able to run. It is also possible that cardiovascular abnormalities in addition to muscle weakness might have limited the ability of the *Zmpste24*$^{-/-}$ mice to run. These preliminary results are in contrast to exercise rescuing the aging phenotype in another mouse model of progeria (Safdar et al. 2011).

Overall, our data support the hypothesis that hindlimb muscles of *Zmpste24*$^{-/-}$ mice have some of the key characteristics of sarcopenia including both muscle atrophy and weakness. We also characterized abnormal joint mechanics, which combined with muscle weakness, likely caused the poor neuromuscular performances by *Zmpste24*$^{-/-}$ mice. We conclude that skeletal muscle is an affected tissue in this progeroid mouse model and it is probable that it is one of the segmented tissues affected in HGPS as well. The identification of skeletal muscle as an affected tissue in progeria lends support to the contention that stem cells, likely satellite cells in this tissue, are fundamentally involved in the segmentation of affected tissues in accelerated aging diseases.

Acknowledgments The authors would like to thank Stephen Young (University of California, Los Angeles) for the gift of *Zmpste24*$^{-/-}$ breeders as well as Greg Cochrane, Trevor Keyler, Allison Kosir, Ron McElmurry, and Brandon Peacock for their contributions to this project. The research was supported by the Progeria Research Foundation (J. Tolar) and National Institute of Health grants K02 -AG036827 (D.A. Lowe) and T32-AR07612 (J.A. Call).

References

Baltgalvis KA, Call JA, Nikas JB, Lowe DA (2009) Effects of prednisolone on skeletal muscle contractility in mdx mice. Muscle Nerve 40:443–454

Bergo MO, Gavino B, Ross J, Schmidt WK, Hong C, Kendall LV, Mohr A, Meta M, Genant H, Jiang Y, Wisner ER, Van Bruggen N, Carano RA, Michaelis S, Griffey SM, Young SG (2002) Zmpste24 deficiency in mice causes spontaneous bone fractures, muscle weakness, and a prelamin A processing defect. Proc Natl Acad Sci U S A 99:13049–13054

Bonne G, Di Barletta MR, Varnous S, Becane HM, Hammouda EH, Merlini L, Muntoni F, Greenberg CR, Gary F, Urtizberea JA, Duboc D, Fardeau M, Toniolo D, Schwartz K (1999) Mutations in the gene encoding lamin A/C cause autosomal dominant Emery–Dreifuss muscular dystrophy. Nat Genet 21:285–288

Brooks SV, Faulkner JA (1988) Contractile properties of skeletal muscles from young, adult and aged mice. J Physiol 404:71–82

Call JA, McKeehen JN, Novotny SA, Lowe DA (2010) Progressive resistance voluntary wheel running in the mdx mouse. Muscle Nerve 42:871–880

Capell BC, Collins FS (2006) Human laminopathies: nuclei gone genetically awry. Nat Rev Genet 7:940–952

Carlson CG, Rutter J, Bledsoe C, Singh R, Hoff H, Bruemmer K, Sesti J, Gatti F, Berge J, McCarthy L (2010) A simple protocol for assessing inter-trial and inter-examiner reliability for two noninvasive measures of limb muscle strength. J Neurosci Methods 186:226–230

De Sandre-Giovannoli A, Bernard R, Cau P, Navarro C, Amiel J, Boccaccio I, Lyonnet S, Stewart CL, Munnich A, Le Merrer M, Levy N (2003) Lamin a truncation in Hutchinson–Gilford progeria. Science 300:2055

Emery AE (2002) The muscular dystrophies. Lancet 359:687–695

Eriksson M, Brown WT, Gordon LB, Glynn MW, Singer J, Scott L, Erdos MR, Robbins CM, Moses TY, Berglund P, Dutra A, Pak E, Durkin S, Csoka AB, Boehnke M, Glover TW, Collins FS (2003) Recurrent de novo point mutations

in lamin A cause Hutchinson–Gilford progeria syndrome. Nature 423:293–298

Faulkner JA, Brooks SV, Zerba E (1995) Muscle atrophy and weakness with aging: contraction-induced injury as an underlying mechanism. J Gerontol A Biol Sci Med Sci 50 (Spec No):124–129

Fielding RA, Vellas B, Evans WJ, Bhasin S, Morley JE, Newman AB, Abellan van Kan G, Andrieu S, Bauer J, Breuille D, Cederholm T, Chandler J, De Meynard C, Donini L, Harris T, Kannt A, Keime Guibert F, Onder G, Papanicolaou D, Rolland Y, Rooks D, Sieber C, Souhami E, Verlaan S, Zamboni M (2011) Sarcopenia: an undiagnosed condition in older adults. Current consensus definition: prevalence, etiology, and consequences. International working group on sarcopenia. J Am Med Dir Assoc 12(4):249–256

Fong LG, Ng JK, Meta M, Cote N, Yang SH, Stewart CL, Sullivan T, Burghardt A, Majumdar S, Reue K, Bergo MO, Young SG (2004) Heterozygosity for LMNA deficiency eliminates the progeria-like phenotypes in Zmpste24-deficient mice. Proc Natl Acad Sci U S A 101:18111–18116

Franklyn PP (1976) Progeria in siblings. Clin Radiol 27:327–333

Frock RL, Kudlow BA, Evans AM, Jameson SA, Hauschka SD, Kennedy BK (2006) Lamin A/C and emerin are critical for skeletal muscle satellite cell differentiation. Genes Dev 20:486–500

Garlich MW, Baltgalvis KA, Call JA, Dorsey LL, Lowe DA (2010) Plantarflexion contracture in the *mdx* mouse. Am J Phys Med Rehabil 89(12):976–985

Gordon LB, McCarten KM, Giobbie-Hurder A, Machan JT, Campbell SE, Berns SD, Kieran MW (2007) Disease progression in Hutchinson-Gilford progeria syndrome: impact on growth and development. Pediatrics 120:824–833

Grattan MJ, Kondo C, Thurston J, Alakija P, Burke BJ, Stewart C, Syme D, Giles WR (2005) Skeletal and cardiac muscle defects in a murine model of Emery–Dreifuss muscular dystrophy. Novartis Found Symp 264:118–133, discussion 133–119, 227–130

Greising SM, Baltgalvis KA, Kosir AM, Moran AL, Warren GL, Lowe DA (2011) Estradiol's beneficial effect on murine muscle function is independent of muscle activity. J Appl Physiol 110:109–115

Halaschek-Wiener J, Brooks-Wilson A (2007) Progeria of stem cells: stem cell exhaustion in Hutchinson–Gilford progeria syndrome. J Gerontol A Biol Sci Med Sci 62:3–8

Hamer L, Kaplan F, Fallon M (1988) The musculoskeletal manifestations of progeria. A literature review. Orthopedics 11:763–769

Hennekam RC (2006) Hutchinson–Gilford progeria syndrome: review of the phenotype. Am J Med Genet A 140:2603–2624

Ingram DK (2000) Age-related decline in physical activity: generalization to nonhumans. Med Sci Sports Exerc 32:1623–1629

Janssen I, Heymsfield SB, Ross R (2002) Low relative skeletal muscle mass (sarcopenia) in older persons is associated with functional impairment and physical disability. J Am Geriatr Soc 50:889–896

Josephson RK (1993) Contraction dynamics and power output of skeletal muscle. Annu Rev Physiol 55:527–546

Lammerding J, Schulze PC, Takahashi T, Kozlov S, Sullivan T, Kamm RD, Stewart CL, Lee RT (2004) Lamin A/C deficiency causes defective nuclear mechanics and mechanotransduction. J Clin Invest 113:370–378

Landisch RM, Kosir AM, Nelson SA, Baltgalvis KA, Lowe DA (2008) Adaptive and nonadaptive responses to voluntary wheel running by mdx mice. Muscle Nerve 38:1290–1303

Leung GK, Schmidt WK, Bergo MO, Gavino B, Wong DH, Tam A, Ashby MN, Michaelis S, Young SG (2001) Biochemical studies of Zmpste24-deficient mice. J Biol Chem 276:29051–29058

Macnamara BG, Farn KT, Mitra AK, Lloyd JK, Fosbrooke AS (1970) Progeria. Case report with long-term studies of serum lipids. Arch Dis Child 45:553–560

Maraldi NM, Capanni C, Del Coco R, Squarzoni S, Columbaro M, Mattioli E, Lattanzi G, Manzoli FA (2011) Muscular laminopathies: role of prelamin A in early steps of muscle differentiation. Adv Enzyme Regul 51(1):246–256

Martin GM (1990) Segmental and unimodal progeroid syndromes of man. In: Harrison DE (ed) Genetic Effect on Aging Vol II. Telford Press, Caldwell, pp 423–520

Merideth MA, Gordon LB, Clauss S, Sachdev V, Smith AC, Perry MB, Brewer CC, Zalewski C, Kim HJ, Solomon B, Brooks BP, Gerber LH, Turner ML, Domingo DL, Hart TC, Graf J, Reynolds JC, Gropman A, Yanovski JA, Gerhard-Herman M, Collins FS, Nabel EG, Cannon RO 3rd, Gahl WA, Introne WJ (2008) Phenotype and course of Hutchinson-Gilford progeria syndrome. N Engl J Med 358:592–604

Moran AL, Warren GL, Lowe DA (2005) Soleus and EDL muscle contractility across the lifespan of female C57BL/6 mice. Exp Gerontol 40:966–975

Moran AL, Warren GL, Lowe DA (2006) Removal of ovarian hormones from mature mice detrimentally affects muscle contractile function and myosin structural distribution. J Appl Physiol 100:548–559

Muchir A, Bonne G, van der Kooi AJ, van Meegen M, Baas F, Bolhuis PA, de Visser M, Schwartz K (2000) Identification of mutations in the gene encoding lamins A/C in autosomal dominant limb girdle muscular dystrophy with atrioventricular conduction disturbances (LGMD1B). Hum Mol Genet 9:1453–1459

Olive M, Harten I, Mitchell R, Beers J, Djabali K, Cao K, Erdos MR, Blair C, Funke B, Smoot L, Gerhard-Herman M, Machan JT, Kutys R, Virmani R, Collins FS, Wight TN, Nabel EG, Gordon LB (2010) Cardiovascular Pathology in Hutchinson-Gilford Progeria: Correlation With the Vascular Pathology of Aging. Arterioscler Thromb Vasc Biol 30:2301–2309

Pekovic V, Hutchison CJ (2008) Adult stem cell maintenance and tissue regeneration in the ageing context: the role for A-type lamins as intrinsic modulators of ageing in adult stem cells and their niches. J Anat 213:5–25

Pendas AM, Zhou Z, Cadinanos J, Freije JM, Wang J, Hultenby K, Astudillo A, Wernerson A, Rodriguez F, Tryggvason K, Lopez-Otin C (2002) Defective prelamin A processing and muscular and adipocyte alterations in Zmpste24 metalloproteinase-deficient mice. Nat Genet 31:94–99

Reddy GK, Enwemeka CS (1996) A simplified method for the analysis of hydroxyproline in biological tissues. Clin Biochem 29:225–229

Rivas D, Li W, Akter R, Henderson JE, Duque G (2009) Accelerated features of age-related bone loss in zmpste24 metalloproteinase-deficient mice. J Gerontol A Biol Sci Med Sci 64:1015–1024

Rodriguez S, Eriksson M (2010) Evidence for the involvement of lamins in aging. Curr Aging Sci 3:81–89

Roos MR, Rice CL, Vandervoort AA (1997) Age-related changes in motor unit function. Muscle Nerve 20:679–690

Safdar A, Bourgeois JM, Ogborn DI, Little JP, Hettinga BP, Akhtar M, Thompson JE, Melov S, Mocellin NJ, Kujoth GC, Prolla TA, Tarnopolsky MA (2011) Endurance exercise rescues progeroid aging and induces systemic mitochondrial rejuvenation in mtDNA mutator mice. Proc Natl Acad Sci 108:4135–4140. doi:10.1073/pnas.1019581108

Scaffidi P, Misteli T (2008) Lamin A-dependent misregulation of adult stem cells associated with accelerated ageing. Nat Cell Biol 10:452–459

Stewart CL, Kozlov S, Fong LG, Young SG (2007) Mouse models of the laminopathies. Exp Cell Res 313:2144–2156

Sullivan T, Escalante-Alcalde D, Bhatt H, Anver M, Bhat N, Nagashima K, Stewart CL, Burke B (1999) Loss of A-type lamin expression compromises nuclear envelope integrity leading to muscular dystrophy. J Cell Biol 147:913–920

Varga R, Eriksson M, Erdos MR, Olive M, Harten I, Kolodgie F, Capell BC, Cheng J, Faddah D, Perkins S, Avallone H, San H, Qu X, Ganesh S, Gordon LB, Virmani R, Wight TN, Nabel EG, Collins FS (2006) Progressive vascular smooth muscle cell defects in a mouse model of Hutchinson–Gilford progeria syndrome. Proc Natl Acad Sci U S A 103:3250–3255